JOURNAL OF SPACECRAFT AND ROCKETS
Vol. 37, No. 4, July–August 2000

# In Situ Oxygen–Atom Erosion Study of Polyhedral Oligomeric Silsesquioxane-Siloxane Copolymer

Rene I. Gonzalez* and Shawn H. Phillips†
*U.S. Air Force Research Laboratory, Edwards Air Force Base, California 93524*
and
Gar B. Hoflund‡
*University of Florida, Gainesville, Florida 32611*

**The surface of a polyhedral oligomeric silsesquioxane-siloxane copolymer film has been characterized in situ by using x-ray photoelectron spectroscopy before and after exposure to incremental fluences of oxygen atoms produced by a hyperthermal oxygen atom source. The data indicate that the atomic oxygen initially attacks the cyclohexyl groups that surround the polyhedral oligomeric silsesquioxane cage, resulting in the formation and desorption of $CO_2$ from the surface. The carbon concentration in the near-surface region is reduced from 65.0 at% for the as-entered surface to 16.3 at% following 63 h of O-atom exposure at a flux of $2 \times 10^{13}$ O atoms/cm$^2$ s. The oxygen and silicon concentrations are increased with incremental exposures to the O-atom flux, but the rates of increase slow with increased exposure. The oxygen concentration increases from 18.5 at% for the as-entered sample to 55.7 at% following the 63-h exposure, and the silicon concentration increases from 16.6 to 28.0 at%. The data reveal the formation of a silica layer on the surface, which serves as a protective barrier preventing further degradation of the underlying polymer with increased exposure to the O-atom flux.**

## Introduction

THE aggressive conditions present in low Earth orbit (LEO) at altitudes ranging from 200 to 700 km in the ionosphere reduce the longevity of organic materials used in the construction of space vehicles, thereby restricting the number of space-certified materials. The predominant environmental species in LEO responsible for this material degradation is atomic oxygen (AO).[1–4] AO is formed by the dissociation of molecular oxygen by ultraviolet radiation from the sun, resulting in an AO concentration of approximately $10^8$ atoms/cm$^3$. The reverse reaction in which an oxygen molecule forms from AO does not have a high reaction rate because it requires a teratomic collision. The third atom is required to carry away the energy released by the formation of $O_2$. For this reason the predominant species in LEO is AO. The actual flux of the impingement of $\sim 10^{15}$ atoms/cm$^2$ s on a spacecraft is high as a result of orbiting speeds of approximately 8 km/s. At these relative speeds AO particles collide with a kinetic energy of $\sim 5$ eV (Refs. 5–7). The effect of AO on spacecraft material degradation has been studied on space-exposed materials (in STS missions and at the NASA Long Duration Exposure Facility, or LDEF)[1,8,9] and in simulation facilities.[10–12] In these studies the samples were analyzed by x-ray photoelectron spectroscopy (XPS) but only after the AO-treated samples were exposed to air. Recent studies have shown that exposure to air chemically alters the reactive surfaces formed during AO exposure.[13,14] Therefore, in situ AO erosion studies of polymers must be performed to avoid artifacts induced by air exposure.

In this study a thin film of polyhedral oligomeric silsesquioxane (POSS)-siloxane copolymer has been characterized in situ by using XPS before and after incremental exposures to the flux produced by an electron-stimulated desorption (ESD) atomic oxygen source.[15] POSS molecules are hybrid inorganic–organic structures synthesized from the self-condensation reactions of alkyl trichlorosilanes. Over the past seven years, Lichtenhan and coworkers[16–20] have focused on incorporating POSS frameworks into traditional polymer systems by means of copolymerization, grafting, and blending processes. Significant property enhancements have been reported for these hybrid polymers, including an increased use temperature, increased toughness, decreased flammability, and increased oxidation resistance. These property enhancements are attributed to the nanolevel interaction of the POSS framework with the polymer matrix. Traditionally, silica fillers have been used in polymer applications requiring alterations in physical and mechanical properties such as tensile strength, abrasion, and fatigue resistance. In addition to numerous property enhancements, POSS polymers have lower densities (1.2–1.5 g/ml) than silica fillers (2.4–2.6 g/ml) (Refs. 21 and 22). Unlike silica fillers, POSS frameworks can be easily functionalized for polymer compatibility without significantly affecting processing conditions. Compared with silica fillers, POSS hybrid polymers are able to impart similar property enhancements, including many not possible with the use of filler technology. Previous studies have also shown that Si-O systems exhibit a superior resistance to AO degradation, partly because of their oxophilicity and high bond strength ($\sim 8$ eV) (Refs. 23 and 24). However, pure siloxane systems have displayed many disadvantages for space applications, including the generation of a volatile cyclic species when exposed to AO that can recondense on optical surfaces.[25] The present study details the results obtained from exposing a POSS-polydimethylsiloxane (PDMS) film to a simulated LEO environment. Specifically, it describes the formation of a protective silica layer with exposure to an O-atom flux. This layer serves as a protective barrier, preventing further degradation of the underlying polymer with increased AO exposure.

## Experimental

### O-Atom Source Characteristics

The ESD source used in this study was developed by Hoflund and Weaver[15] and is commercially available through Atom Sources, Inc. It is ultrahigh vacuum (UHV) compatible, operates with the sample at room temperature, and produces a high-purity, hyperthermal, AO flux with an O atom:$O^+$ ratio of $\sim 10^8$. These sources are superior to plasma sources in that they produce hyperthermal, ground-state O atoms and operate at UHV pressures ($\sim 10^{-9}$ torr) with negligible amounts of other species, including ions, contaminants, and UV radiation. The operational concept of the hyperthermal oxygen atom generator is shown in Fig. 1. Ultrahigh-purity molecular $O_2$ dissociatively adsorbs on a metallic Ag alloy membrane at the high-pressure side and permeates at elevated temperature ($\sim 400$°C) to the UHV side. There the adsorbed atoms are struck by a directed flux of primary electrons, which results in ESD of O atoms forming

Received 1 September 1999; revision received 20 January 2000; accepted for publication 24 January 2000. 

*Research Scientist, Propulsion Materials Application Branch.
†Project Leader, Propulsion Materials Application Branch.
‡Professor, Department of Chemical Engineering.

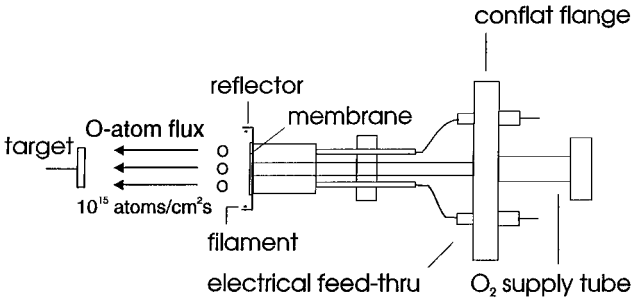


**Fig. 1 Schematic diagram of the atom source.**

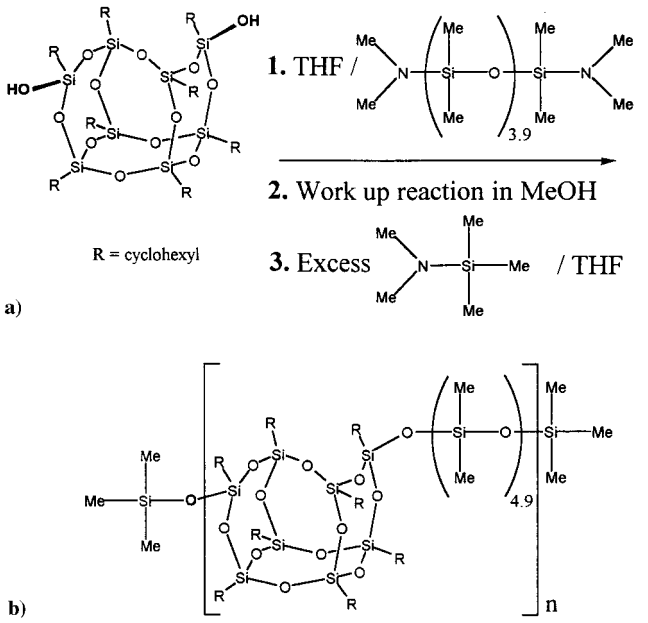


**Fig. 2 Scheme for synthesis of the POSS-PDMS copolymer used in this study.**

a continuous flux. Many processes have to function in series at sufficiently high rates for the system to work, including dissociative adsorption of the molecular gas on the metal surface, permeation of atoms through the membrane, and formation of the neutral flux by ESD. Some bremstrahlung radiation is produced by the electrons' striking the Ag membrane. Because the UV component is small, this radiation has only a small effect on the chemical processes occurring at the sample surface. Another potential problem is the sublimation of Ag from the membrane surface, which could accumulate on the sample surface. Studies have been performed to optimize the power input to the membrane surface so that the O flux is maximized while the Ag sublimation rate is negligible. This is possible because the Ag sublimation rate decreases exponentially with temperature.

The O atoms produced by this source have been shown to be hyperthermal, but their energy distribution has not been measured. Corallo et al.[26] measured the energy distribution of O ions emitted by ESD from a Ag (110) surface and found that this distribution has a maximum of ~5 eV and a full width at half-maximum of 3.6 eV. This ion energy distribution would set an upper bound for the neutral energy distribution because ESD neutrals are generally believed to be less energetic than ESD ions. This point has been discussed often in the ESD literature but not actually demonstrated. A mass spectrometer has been used to characterize the flux produced by this ESD source. The ion acceleration potential was set at 0.0 V in these studies. Because calibration studies demonstrated that the ions entering the quadrupole section had to have a minimum kinetic energy of 2.0 eV to reach the detector, the ESD neutrals have a minimum energy of 2 eV. Therefore, the hyperthermal AO produced by this ESD source has an energy higher than 2 eV but lower than the ion energy distribution.

### Preparation of the POSS-PDMS Copolymer

The POSS siloxane copolymer used in this study and shown in Fig. 2a was synthesized by using a method similar to that described by Lichtenhan et al.[27] and Gilman et al.[28] The diol-silsesquioxane monomer (5.00 g or 4.54 mmol) shown in Fig. 2b was dissolved in 10 ml of tetrahydrofuran (THF) in a 50-ml flask to which 1.98 g (4.54 mmol) of bis(dimethylamino)polydimethylsiloxane (approximately 4.9 silanes per oligomer, $Mw$ = 435.5 g/mol) was added with an additional 15 ml of THF. The reaction mixture was stirred and heated to 65°C under nitrogen for 48 h. The polymer was then precipitated into 350 ml of methanol, stirred for 2 h, and filtered and air dried for 12 h. To end cap the polymer with trimethylsilane, it was dissolved in 25 ml of THF with an excess of *N*, *N*-(dimethylamino) trimethylsilane and reacted at 65°C under nitrogen for another 48 h. The polymer was again precipitated into 350 ml of methanol. After decanting the solvent, fresh methanol with dilute HCl was added to neutralize any excess amine. The solution was again decanted, and the remaining white solid was dried under vacuum for 2 h, producing a yield of 6.27 g (95% theoretical yield). Molecular weights were determined from multiangle laser light-scattering measurements obtained from a DAWN-F detector (Wyatt Technologies) equipped with a gel-permeation chromatography column. The number average molecular weight, mass average molecular weight, and degree of polymerization were found to be 62,000, 118,000, and 43, respectively. A peak area analysis of the $^{29}$Si nuclear magnetic resonance (NMR) data gives a degree of polymerization of 38 and shows on average 4.8 $SiOMe_2$ groups per repeat unit. Relevant peaks in the $^{29}$Si NMR spectrum are a singlet at 7.2 parts in $10^3$ (ppm) ($Me_3Si$ endgroups, peak area of 2.0); a multiplet at 21.5 ppm ($Me_2Si$-O, peak area of 184); and four singlets at 66.39, 68.13, 68.20, and 69.51 ppm (POSS, peak area of 305.6).

### Preparation of Thin Films by Solvent Casting

Thin films of the trimethylsilane-terminated POSS-PDMS were made by dissolving 100 mg of the coarse powder in 15–20 ml of THF, solvent casting onto 1 × 1 cm aluminum substrates, and drying at room temperature for 24 h. The aluminum substrates were prepared and cleaned with Boraxo soap and water, and then deionized water followed by ultrasonic cleaning in toluene, acetone, trichloroethylene, acetone, and ethanol, respectively.

### Surface Characterization

A solvent-casted POSS-PDMS film was wiped with isopropanol and inserted into the UHV chamber (base pressure $< 10^{-10}$ torr). XPS was performed by using a double-pass cylindrical mirror analyzer (DPCMA; PHI Model 25-270AR). XPS survey spectra were taken in the retarding mode with a pass energy of 50 eV, and high-resolution XPS spectra were taken with a pass energy of 25 eV by using Mg K$\alpha$ x-rays (PHI Model 04-151 x ray source). Data collection was accomplished by using a computer interfaced, digital pulse-counting circuit[29] followed by smoothing with digital-filtering techniques.[30] The sample was tilted 30 deg off the axis of the DPCMA, and the DPCMA accepted electrons emitted into a cone 42.6 ± 6 deg off the DPCMA axis.

XPS spectra were first obtained from the as-entered, solvent-cleaned sample. The sample was then transferred by means of a magnetically coupled rotary–linear manipulator into an adjoining UHV chamber that houses the ESD AO source. There the surface was exposed to the hyperthermal AO flux and reexamined without air exposure after total exposure times of 2, 24.6, and 63 h. The approximate normal distance between the sample face and source in this study was 15 cm, at which distance the flux was approximately $2 \times 10^{13}$ atoms/cm$^2$ s for the instrument settings used. The substrate temperature was determined with a chrome-alumel thermocouple attached to the Al substrate. At this distance the sample remained at room temperature during the AO exposures. The sample temperature did increase to 50°C during XPS data collection. After the 63-h AO exposure, the sample was exposed to air (room temperature ~22°C and relative humidity ~60%) for 4.75 h and again examined by using XPS.

## Results and Discussion

XPS survey spectra obtained from a solvent-wiped POSS-PDMS surface before and after the 2-, 24.6-, and 63-h AO exposures are shown in Figs. 3a–3d, respectively. Spectrum e in Fig. 3 was taken after the 4.75-h air exposure following the 63-h AO treatment. The peak assignments shown in Fig. 4 pertain to all five spectra. The predominant peaks apparent in these spectra include the C 1*s*, O 1*s*, Si 2*p*, Si 2*s*, O 2*s*, and O Auger peaks. No Ag features are apparent in these spectra. Significant changes in relative peak heights are observed for the C, O, and Si features following the O-atom exposures. An estimate of the near-surface compositions has been calculated from the peak areas in the survey spectra by assuming that this region is homogeneous and by using published atomic sensitivity factors.[31] The compositions determined in this manner are presented in Table 1 for the as-entered, AO-exposed, and air-exposed surfaces. XPS probes the near-surface region of the sample and yields a weighted average composition, with the atomic layers near the surface being weighted more heavily because these photoemitted electrons have a lower probability of scattering inelastically. The sampling depth is ~30 atomic layers, and ~10% of the signal originates from the outermost atomic layer.[32] This near-surface region is nonhomogeneous because the AO reacts with the outermost few atomic layers. Therefore, the region that is affected to the greatest extent as a result of the reaction with AO also makes the largest contribution to the XPS signal. This fact implies that XPS is an excellent technique for studying the AO erosion of spacecraft materials. Even though the distribution functions involving the depth of chemical reactions in the near-surface region and the XPS determination of the weighted average composition of the near-surface region are complex, the compositional values, determined by using the homogeneous assumption and shown in Table 1 as a function of AO fluence, provide a trend that is indicative of the chemical alterations occurring during AO exposure. This trend is supported by the chemical state alterations determined by XPS, which are discussed next. The O-to-Si atomic ratio is 1.11 for the as-entered sample; it is increased to 1.90 after the 2-h exposure, then reduced to 1.70 after 24.6 h, and increased again to 1.99 after the 63-h O-atom exposures. This behavior indicates that complex chemical reactions occur during AO exposure. After the 4.75-h air exposure the O-to-Si atomic ratio is 1.91. These changes in the O-to-Si atomic ratio resulting from exposure to the AO flux indicate the formation of $SiO_2$ and are consistent with the high-resolution spectra that follow. A large reduction in the C 1*s* peak is observed as a result of the incremental exposures to the AO flux. The near-surface C concentration decreases from 65.0 at% for the as-entered sample to 16.3 at% after the 63-h exposure. This decrease is caused by the reaction of C in the near-surface region with O to form $CO_2$. A small increase in the carbon content to 19.5 at% is observed after exposure to air for 4.75 h, probably as a result of the adsorption of C-containing molecules such as hydrocarbons from the air. Hydrogen in the POSS-PDMS would also react with the AO to form water, which would desorb.

**Table 1 Near-surface composition determined from XPS data obtained from the as-entered, solvent-cleaned, and AO and air-exposed POSS-PDMS sample**

| Surface sample treatment | AO fluence, O/cm$^2$ | Composition, at% O | C | Si | Atom ratio O/Si |
|---|---|---|---|---|---|
| As entered, solvent cleaned | —— | 18.5 | 65.0 | 16.6 | 1.11 |
| 2-h AO exposure | $1.44 \times 10^{17}$ | 33.8 | 48.4 | 17.8 | 1.90 |
| 24.6-h AO exposure | $1.77 \times 10^{18}$ | 49.1 | 22.1 | 28.8 | 1.70 |
| 63-h AO exposure | $4.53 \times 10^{18}$ | 55.7 | 16.3 | 28.0 | 1.99 |
| 4.75-h air exposure following the 63-h AO exposure | $4.53 \times 10^{18}$ | 52.8 | 19.5 | 27.7 | 1.91 |

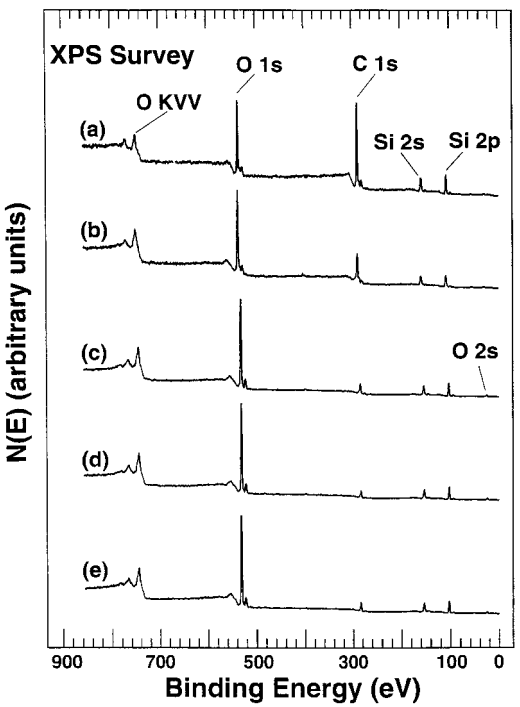


**Fig. 3 XPS survey spectra obtained from a solvent-cleaned, POSS-PDMS film after a) insertion into the vacuum system; b) 2-h, c) 24.6-h, and d) 63-h exposures to the hyperthermal AO flux; and e) 4.75-h air exposure following the 63-h AO exposure.**

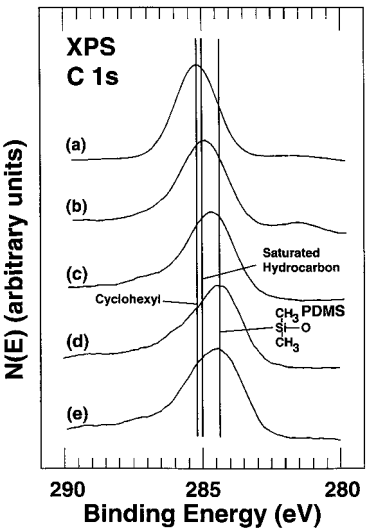


**Fig. 4 XPS C 1*s* spectra obtained from a solvent-cleaned, POSS-PDMS film after a) insertion into the vacuum system; b) 2-h, c) 24.6-h, and 63-h exposures to the hyperthermal AO flux; and e) 4.75-h air exposure following the 63-h AO exposure.**

High-resolution XPS C 1*s*, O 1*s*, and Si 2*p* obtained from the as-received, solvent-wiped surface before and after the 2-, 24.6-, and 63-h AO exposures are shown in spectra a–d of Figs. 4, 5, and 6, respectively. Spectrum e was obtained after the 4.75-h air exposure following the 63-h O-atom exposure. Variations in peak shapes and positions are observed between the nonexposed, AO-exposed, and air-exposed surfaces, indicating that the chemical species distribution is altered by exposure to the AO flux and then to air.

The C 1*s* peak shown in Fig. 4a is centered at 285.2 eV, indicating that the predominant form of carbon present for the as-entered sample is in the form of a fully substituted hydrocarbon, that is, the cyclohexyl groups on the POSS cage.[33] In spectra b, c, and d the C 1*s* peak becomes broader, and the peak center shifts to a lower binding energy (BE) with increasing exposure to the AO flux. After the 63-h exposure, the C 1*s* has a BE of 284.4 eV. This value is characteristic of methyl groups on the PDMS chain.[33] The fact that these changes coincide with a decrease in the total carbon concentration in the near-surface region from 64.1 to 13.5 at% implies that the cyclohexyl groups are being removed selectively, leaving the methyl groups. This selective removal is caused by the larger size of the POSS cage (1.5 nm) compared with the PDMS chain as

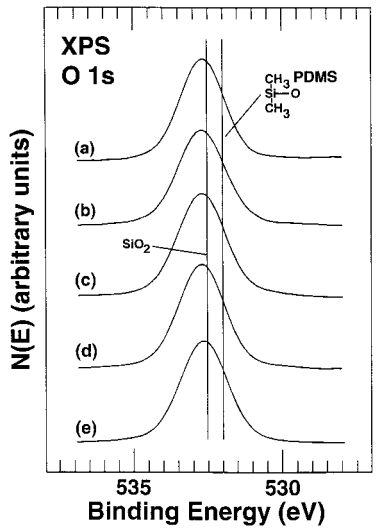


**Fig. 5 XPS O 1*s* spectra obtained from a solvent-cleaned, POSS-PDMS film after a) insertion into the vacuum system; b) 2-h, c) 24.6-h, and d) 63-h exposures to the hyperthermal AO flux; and e) 4.75-h air exposure following the 63-h AO exposure.**

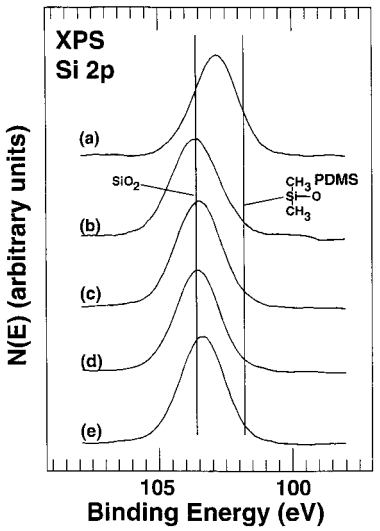


**Fig. 6 XPS Si 2*p* spectra obtained from a solvent-cleaned, POSS-PDMS film after a) insertion into the vacuum system; b) 2-h, c) 24.6-h, and d) 63-h exposures to the hyperthermal AO flux; and e) 4.75-h air exposure following the 63-h AO exposure.**

shown in Fig. 2. Small shoulders are visible on the high-BE side of the C 1*s* peak in spectra b, c, and d. These probably are from species such as alcohols, formaldehydes (BE ~286.0–287.7 eV), and organic acids (BE ~287.5) that form by reaction with the AO flux. Exposure to air (spectrum e) produces an increase in the shoulder near 285.0 eV, indicating adsorption of hydrocarbons from the air at reactive surface sites produced during the AO exposure. This observation is consistent with the increase in the C concentration after the air exposure, as shown in Table 1.

The O 1*s* spectra obtained from the sample before and after the various treatments are shown in Fig. 5. These peaks are broad, indicating that various chemical states of oxygen are present. After the 2-h exposure to the AO flux, the contribution from oxygen is significantly increased from 18.5 to 33.8 at%, and then it increases further to 49.1 and 55.7 at% after the 24.6- and 63-h exposures, respectively. However, the peak shapes and positions do not change much with treatment indicating that the O-containing species have closely spaced O 1*s* BEs. A previous XPS study of PDMS has shown that the oxygen in the PDMS chain has a BE of 532.0 eV (Ref. 33), whereas $SiO_2$ has a BE of ~532.5 eV (Ref. 33).

The Si 2*p* peaks obtained from the sample before and after the various treatments are shown in Fig. 6. Similar to the O 1*s* peak, the Si 2*p* peak for the as-entered sample (spectrum a) is broad, indicating the presence of several chemical states of silicon. This peak is centered at a BE of 102.7 eV, which corresponds to $RSiO_{1.5}$ in the POSS cage. However, spectra b, c, and d reveal the formation of a $SiO_2$ layer with incremental exposures to the AO flux. The fact that little difference is observed in the spectra obtained after the 24.6- and 63-h exposures indicates that this silica layer forms a protective barrier on the surface that prevents further degradation of the polymer with longer exposure to the AO flux. The significant compositional changes observed indicate that most of the near-surface region examined by XPS is altered by the AO exposure. The chemical reactions that form $CO_2$ and $H_2O$ are exothermic so that the local surface temperature may be relatively high. This fact and the fact that the AO provides a chemically induced driving force at the surface result in diffusion of subsurface C and H to the surface where they react with the AO. This mechanism is responsible for the subsurface compositional alterations observed by using XPS and for the formation of a relatively thick $SiO_2$ layer.

## Conclusion

The surface of a POSS-PDMS copolymer film has been characterized in situ by using XPS before and after exposure to different fluences of AO produced by an ESD hyperthermal oxygen atom source. The XPS data indicate that the carbon content of the near-surface region is decreased from 65.0 to 16.3 at% after a 63-h exposure to an AO flux of $2 \times 10^{13}$ atoms/cm$^2$ s. The oxygen and silicon concentrations in the near-surface region increase with increasing exposure to the AO flux, with the oxygen-to-silicon atom ratio increasing from 1.11 for the as-entered sample to 1.99 after a 63-h AO exposure. High-resolution XPS data suggest that the AO initially attacks the cyclohexyl groups on the POSS cage forming $CO_2$ and $H_2O$, which desorb. Increased exposure to the AO flux results in the formation of a silica layer on the surface, which acts a protective barrier preventing further degradation of the underlying polymer.

## Acknowledgments

Funding for this research was received from the Air Force Office of Scientific Research, Directorate of Chemistry and Life Sciences. The authors appreciate the efforts of Tim Haddad with regard to polymer synthesis and technical advice from Kevin Chaffee.

## References

[1]Koontz, S. L., Leger, L. J., Visentine, J. T., Hunton, D. E., Cross, J. B., and Hakes, C. L., "EOIM-III Mass Spectroscopy and Polymer Chemistry: STS 46, July–August 1992," *Journal of Spacecraft and Rockets*, Vol. 32, No. 3, 1995, pp. 483–495.

[2]Cross, J. B., Koontz, S. L., and Hunton, D. E., "Flight Mass-Spectrometer Calibration in a High-Velocity Atomic-Oxygen Beam," *Journal of Spacecraft and Rockets*, Vol. 32, No. 3, 1995, pp. 496–501.

[3]Champion, K. S. W., Cole, A. E., and Kantor, A. J., "Standard and Reference Atmospheres," *Handbook of Geophysics and the Space Environment*, edited by A. S. Jursa, Air Force Geophysics Lab., U.S. Air Force (National Technical Information Service), Springfield, VA, 1985, pp. 14-1–14-43.

[4]Hedin, A. E., "A Revised Thermospheric Model Based on Mass Spectrometer and Incoherent Scatter Data: MSIS-83," *Journal of Geophysical Research*, Vol. 88, No. A12, 1983, pp. 10,170–10,188.

[5]Reddy, M. R., "Review: Effect of Low Earth Orbit Atomic Oxygen on Spacecraft Materials," *Journal of Materials Science*, Vol. 30, No. 2, 1995, pp. 281–307.

[6]Packirisamy, S., Schwam, D., and Litt, M. H., "Review: Atomic Oxygen Resistant Coatings for Low Earth Orbit Space Structures," *Journal of Materials Science*, Vol. 30, No. 2, 1995, pp. 308–320.

[7]Reddy, M. R., Srinivasamurthy, N., and Agrawal, B. L., "Effect of the Low-Earth-Orbit Atomic-Oxygen Environment on Solar-Array Materials," *European Space Agency Journal*, Vol. 16, No. 2, 1992, pp. 193–208.

[8]de Groh, K. K., and Banks, B. A., "Atomic-Oxygen Undercutting of Long Duration Exposure Facility Aluminized-Kapton Multilayer Insulation," *Journal of Spacecraft and Rockets*, Vol. 31, No. 4, 1994, pp. 656–664.

[9]Banks, B. A., Rutledge, S. K., de Groh, K. K., Mirtich, M. J., Gebauer, L., Olle, R., and Hill, C. M., "The Implication of the LDEF Results on Space Freedom Power System Materials," *Proceedings of the 5th International Symposium on Materials in a Space Environment*, Cannes-Madelieu, France, 1991, p. 137.

[10]Tennyson, R. C., "Atomic Oxygen Effects on Polymer-Based Materials," *Canadian Journal of Physics*, Vol. 69, No. 9, 1991, pp. 1190–1208.

[11]Cazaubon, B., Paillous, A., Siffre, J., and Thomas, R., "Five-Electron-Volt Atomic Oxygen Pulsed-Beam Characterization by Quadrupolar Mass Spectrometry," *Journal of Spacecraft and Rockets*, Vol. 33, No. 6, 1996, pp. 870–876.

[12]de Groh, K. K., Terlep, J. A., and Dever, T. M., "Atomic Oxygen Durability of Solar Concentrator Materials for Space Station Freedom," NASA TM-105378, Sept. 1990.

[13]Grossman, E., Lifshitz, Y., Wolan, J. T., Mount, C. K., and Hoflund, G. B., "In Situ Erosion Study of Kapton Using Novel Hyperthermal Oxygen Atom Source," *Journal of Spacecraft and Rockets*, Vol. 36, No. 1, 1999, pp. 75–78.

[14]Wolan, J. T., and Hoflund, G. B., "Chemical and Structural Alterations Induced at Kapton Surfaces by Air Exposure Following Atomic Oxygen or 1 keV $Ar^+$ Treatments," *Journal of Vacuum Science and Technology A*, Vol. 17, No. 2, 1999, pp. 662–664.

[15]Hoflund, G. B., and Weaver, J. F., "Performance Characteristics of a Hyperthermal Oxygen Atom Generator," *Measurement Science and Technology*, Vol. 5, No. 3, 1994, pp. 201–205.

[16]Mather, P. T., Jeon, H. G., Romo-Uribe, A., Haddad, T. S., and Lichtenhan, J. D., "Mechanical Relaxation and Microstructure of Poly(norbornyl-POSS) Copolymers," *Macromolecules*, Vol. 32, No. 4, 1999, pp. 1194–1203.

[17]Lee, A., and Lichtenhan, J. D., "Viscoelastic Responses of Polyhedral Oligosilsesquioxane Reinforced Epoxy Systems," *Macromolecules*, Vol. 31, No. 15, 1998, pp. 4970–4974.

[18]Haddad, T. S., and Lichtenhan, J. D., "Hybrid Organic-Inorganic Thermoplastics: Styryl-Based Polyhedral Oligomeric Silsesquioxane Polymers," *Macromolecules*, Vol. 29, No. 22, 1996, pp. 7302–7304.

[19]Haddad, T. S., Choe, E., and Lichtenhan, J. D., "Hybrid Styryl-Based Polyhedral Oligomeric Silsesquioxane (POSS) Polymers," *Materials Research Society Proceedings*, Vol. 435, 1996, pp. 25–32.

[20]Lichtenhan, J. D., Noel, C. J., Bolf, A. G., and Ruth, P. N., "Thermoplastic Hybrid Materials: Polyhedral Oligomeric Silsesquioxane (POSS) Reagents, Linear Polymers, and Blends," *Materials Research Society Proceedings*, Vol. 435, 1996, pp. 3–11.

[21]Olsson, K., "An Improved Method to Prepare Octa-(alkylsilsesquioxanes) $(RSi)_8O_{12}$," *Arkiv För Kemi*, Vol. 13, No. 37, 1958, pp. 367–378.

[22]Strong, A. B., *Fundamentals of Composites Manufacturing: Materials, Methods, and Applications*, edited by C. A. Ploskona, Society of Manufacturing Engineers, Dearborn, MI, 1989, p. 39.

[23]Taylor, G. N., and Wolf, T. M., "Oxygen Plasma Removal of Thin Polymer Films," *Polymer Engineering and Science*, Vol. 20, No. 16, 1980, pp. 1087–1092.

[24]Connell, J. W., Crivello, J. V., and Bi, D., "Effect of Low Earth Orbit Atomic Oxygen Exposure on Epoxy Functionalized Siloxanes," *Journal of Applied Polymer Science*, Vol. 57, No. 10, 1995, pp. 1251–1259.

[25]Thorne, J. A., and Whipple, C. L., "Silicones in Outer Space," *The Effects of the Space Environment on Materials*, Society of Aerospace Material and Process Engineers, North Hollywood, CA, 1967, pp. 243–253.

[26]Corallo, G. R., Hoflund, G. B., and Outlaw, R. A., "An Energy-Resolved Electron Stimulated Desorption (ESD) Study of Oxygen-Exposed Ag(110)," *Surface and Interface Analysis*, Vol. 12, Dec. 1988, pp. 185–190.

[27]Lichtenhan, J. D., Vu, N. Q., Carter, J. A., Gilman, J. W., and Feher, F. J., "Silsesquioxane-Siloxane Copolymers from Polyhedral Silsesquioxanes," *Macromolecules*, Vol. 26, No. 8, 1993, pp. 2141, 2142.

[28]Gilman, J. W., Schlitzer, D. S., and Lichtenhan, J. D., "Low Earth Orbit Resistant Siloxane Copolymers," *Journal of Applied Polymer Science*, Vol. 60, No. 4, 1996, pp. 591–596.

[29]Gilbert, R. E., Cox, D. F., and Hoflund, G. B., "Computer-Interfaced Digital Pulse Counting Circuit," *Review of Scientific Instruments*, Vol. 53, No. 8, 1982, pp. 1281–1284.

[30]Savitzky, A., and Golay, M. J. E., "Smoothing and Differentiation of Data by Simplified Least Squares Procedures," *Analytical Chemistry*, Vol. 36, No. 8, 1964, pp. 1627–1639.

[31]Wagner, C. D., Riggs, W. M., Davis, L. E., Moulder, J. F., and Muilenberg, G. E. (eds.), *Handbook of X-Ray Photoelectron Spectroscopy*, Perkin–Elmer Corp., Eden Prairie, MN, 1979, p. 188.

[32]Hoflund, G. B., "Spectroscopic Techniques: X-Ray Photoelectron Spectroscopy (XPS), Auger Electron Spectroscopy (AES) and Ion Scattering Spectroscopy (ISS)," *Handbook of Surface and Interface Analysis: Methods in Problem Solving*, edited by J. C. Rivière, and S. Myhra, Marcel Dekker, New York, 1998, pp. 57–158.

[33]Beamson, G., and Briggs, D., *High Resolution XPS of Organic Polymers: The Scienta ESCA300 Database*, Wiley, New York, 1992, pp. 268, 269.

A. C. Tribble
*Associate Editor*